Oxygen and chlorine electrodes on semiconductive SnO_2 in molten LiCl - KCl eutectic

I. UCHIDA, S. TOSHIMA

Department of Applied Chemistry, Faculty of Engineering, Tohoku University, Sendai 980, Japan

The oxidation of oxide (O^{2-}) and chloride ions were studied at tin oxide electrodes in molten LiCl–KCl eutectic at 450° C using voltammetric techniques. The polarization characteristics of the oxide semiconductor electrode were compared with that of Pt in the case of the oxygen electrode and with that of glassy carbon in the case of chlorine evolution. Both electrode reactions on tin oxide were found to be somewhat less reversible compared with the results of Pt and GC. It is suggested that the observed irreversibility is related to the electron tunnelling process through the space charge barrier formed at the semiconductor surface.

1. Introduction

Sb-doped tin oxide films prepared on Pyrex substrates are usable as stable anode materials in molten LiCl–KCl eutectic as indicated previously [1, 2]. The SnO_2–melt interface has been characterized by semiconductor–liquid junction theory for an n-type semiconductor, where the flat band potential (E_{fb}) was estimated as -1.29 V versus 1 M Pt(II)/Pt at 450° C [1]. Accordingly the space charge barrier depleted in electron concentration is formed inside the electrode at more negative potentials than E_{fb}. However, for a highly doped electrode whose doping level was about 10^{20} cm^{-3}, the space charge barrier has been shown experimentally to be transparent to electrons due to tunnelling [2].

In the present paper, the electro-oxidation of Cl^- and O^{2-} have been examined on SnO_2 electrodes in molten LiCl–KCl eutectic at 450° C, and compared with their oxidation reactions on Pt and glassy carbon electrodes.

2. Experimental

Tin oxide films were prepared on Pyrex substrates by a spray method. The preparation and construction of the electrodes usable in molten salt systems were described previously [1–3]. Glassy carbon (GC) and platinum were also used as working electrodes for comparison. The construction of Pt flag

electrodes [4] and GC electrodes sealed into Pyrex tubes [5] was described elsewhere.

In the study of the chlorine electrode, Pyrex glassware was used for the electrochemical cell assembly as described in a previous paper [4]. The counter electrode was a spectroscopic grade graphite rod, and the reference electrode was a Pt(II)/Pt electrode. Both electrodes were separated from the working electrode by fine fritted discs.

In the study of the oxygen electrode, an alumina crucible SSA-S (Nippon Kagaku Togyo Co) was used as the melt container in order to avoid O^{2-} consumption by the Pyrex wall. The glass compartments were not placed in the melt container, only a carbon rod as the counter electrode and a thin tip of Pyrex membrane–Ni(II)/Ni reference electrode [6] being in contact with the melt. The Ni(II)/Ni reference electrode potential was measured against the Pt(II)/Pt reference electrode.

Molten LiCl–KCl eutectic was prepared from the AR grade reagents and purified using dry HCl treatment and pre-electrolysis [1]. Chlorine from cylinders (Hodogaya Kagaku Co) was purified by passing it over anhydrous $Mg(ClO_4)_2$. The concentration of O^{2-} was changed by adding Li_2O (Research Organic/Inorganic Chemical Corp. 99% pure) with a special apparatus called a powder burette, which was described previously [2].

All potentials in this paper are quoted with respect to the 1 M Pt(II)/Pt reference electrode,

and all experiments were carried out at 450° C, the temperature being monitored by a digital thermometer TR-2112 (Takeda Riken Kogyo Co) and a Chromel-Alumel thermocouple. The electro-oxidation of O^{2-} was examined under an atmospheric pressure of purified argon by cyclic voltammetry. Chlorine evolution was carried out under an atmospheric pressure of chlorine by measuring electrode potentials at constant current conditions.

3. Results and discussion

3.1. Oxygen electrode

The voltammetric waves of O^{2-} oxidation obtained at a SnO$_2$ electrode are shown in Fig. 1. For comparison, corresponding voltammograms at a Pt electrode are shown in Fig. 2. According to Kanzaki et al. [7], the oxidation of O^{2-} on Pt gives reversible voltammograms with $n = 2$. Comparing Fig. 1 with Fig. 2, it can be seen that the waves at SnO$_2$ are broadened and the peak separation is larger than that of Pt. This irreversibility is mainly due to the effect of iR-drop, because the electrical resistance along the thin SnO$_2$ film on the substrate is relatively large. The resistance depends on the electrode construction and sometimes with highly resistive SnO$_2$ electrodes the anodic peak was not well defined.

According to the theory of cyclic voltammetry [8], and including the ohmic drop, the following expressions may be written for the reversible case

$$E_p - E_{p/2} = 2 \cdot 199 \, RT/nF + 0 \cdot 5 i_p R \quad (1)$$
$$E_{0 \cdot 8517 i_p} = E_{1/2} + 0 \cdot 8517 i_p R \quad (2)$$

where $2 \cdot 199 \, RT/nF$ is $0 \cdot 137/n$ V at 450° C. Although these equations are not rigorous, they may be used to remove the iR-drop. In the case of Pt electrodes, the resistance R is close to zero, then the n value and $E_{1/2}$ are obtained using experimental values of E_p and $E_{p/2}$; $n = 1 \cdot 96$ and $E_{1/2} = -0 \cdot 546$ V versus 1 M Pt(II)/Pt.

Assuming reversible electron transfer at the SnO$_2$ electrodes, the $(E_p - E_{p/2})$ versus i_p plot is linear, leading to the evaluation of n and R in Equation 1. In addition the $E_{1/2}$ obtained from $E_{0 \cdot 8517 i_p}$ versus i_p plots should be equal to the $E_{1/2}$ obtained at Pt. Those plots are shown in Fig. 3, yielding $n = 1 \cdot 7$ and $E_{1/2} = -0 \cdot 54 \pm 0 \cdot 01$ V versus 1 M Pt(II)/Pt. Consequently, it may be concluded that the electro-oxidation of O^{2-} takes place on SnO$_2$ in a quasi-reversible manner with $n = 2$. Although the reaction on SnO$_2$ is somewhat less reversible than that on Pt, the oxidation processes on both electrodes seem to be essentially identical, indicating no specific or catalytic effects at the metal or the oxide surfaces.

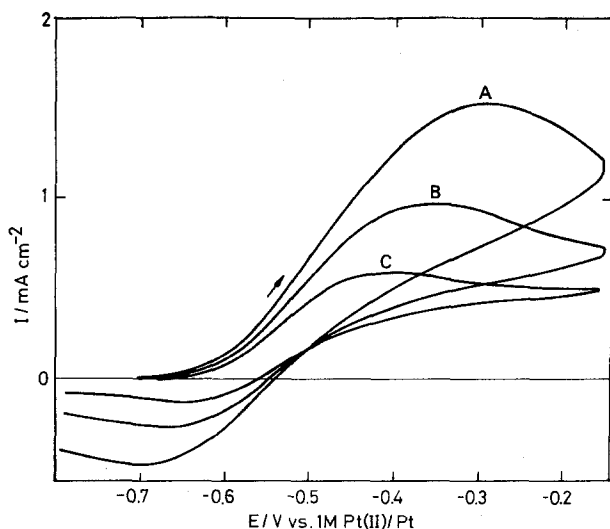Plots of i_p versus the square root of the scan rate were linear at various concentrations of O^{2-},

Fig. 1. Cyclic voltammograms for oxidation of O^{2-} at SnO$_2$ electrode in LiCl–KCl eutectic (450° C) containing 4·9 mM Li$_2$O: scan rates (A) 0·10 V s^{-1}, (B) 0·05 V s^{-1}, (C) 0·02 V s^{-1}.
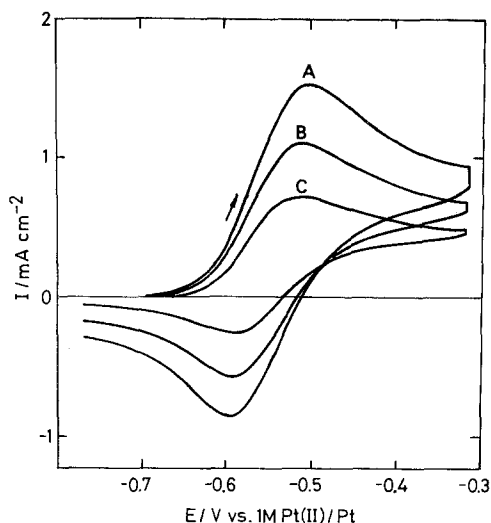
Fig. 2. Cyclic voltammograms for oxidation of O^{2-} at Pt electrode in LiCl–KCl eutectic (450° C) containing 4·9 mM Li_2O: scan rates (A) 0·10 V s⁻¹, (B) 0·05 V s⁻¹, (C) 0·02 V s⁻¹.
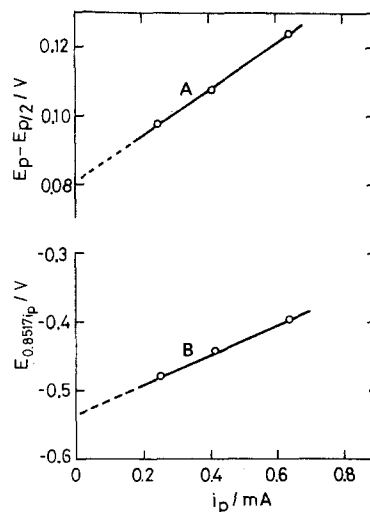
Fig. 3. Correction for ohmic voltage drop due to electrode resistance of SnO₂ in determination of $(E_p - E_{p/2})$ and $E_{1/2}$ of Fig. 1. (A) $(E_p - E_{p/2})$ versus i_p plot, (B) E at $0·8517i_p$ versus i_p plot.

indicating diffusion control for the oxidation. However, the values of $i_p/v^{1/2}$ for SnO₂ were smaller than those for Pt at the same concentration of O^{2-}. This discrepancy can be attributed to the decrease of peak current due to the effect of uncompensated electrode resistance. The diffusion coefficient of O^{2-} in LiCl–KCl eutectic at 450° C was calculated by using the expression for the reversible case [8]

$$i_p = 1·73 \times 10^2 n^{3/2} A D^{1/2} c v^{1/2} \qquad (3)$$

where i_p is the peak current (A), n the number of electrons, A the area of electrode (cm^2), D the diffusion coefficient ($cm^2 s^{-1}$), C the concentration (M), and v the scan rate (V s⁻¹). The results are summarized in Table 1.

Table 1. Diffusion coefficients of O^{2-} in LiCl–KCl at 450° C

Concentration (mM)	$D \times 10^6$/Pt ($cm^2 s^{-1}$)	$D \times 10^6$/SnO₂ ($cm^2 s^{-1}$)
1·0	4·4	
4·9	4·8	3·5
12·9		4·4*

* measured with an *iR*-compensator

The values of D in the literature are $2·4 \times 10^{-6}$ $cm^2 s^{-1}$ at 400° C [7], $2·8 \times 10^{-6}$ and $7·0 \times 10^{-6}$ $cm^2 s^{-1}$ at 390° C and 480° C, respectively [9]. Our average for D, $4·5 \times 10^{-6} cm^2 s^{-1}$, is in reasonable agreement with the above.

There is a contradiction in the mechanism of the oxygen electrode in LiCl–KCl eutectic [10]. Inman et al. suggested the participation of peroxide ion in the reaction [11]. Kanzaki et al., however, demonstrated that peroxide and superoxide ions are unstable in the melt [12], yielding oxide ions due to their decomposition, and proposed a simple mechanism consisting of a reversible two-electron transfer process followed by a slow dimerization reaction [7]

$$O^{2-} = O + 2e^- \qquad (4)$$

$$O + O \longrightarrow O_2. \qquad (5)$$
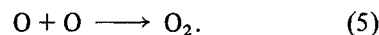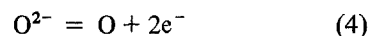
According to the diagnostic criteria of Nicholson and Shain [8], the ratio of cathodic to anodic peak current i_c/i_a shows a levelling off at a value of 1·0 with decreasing scan rate, if a reversible charge transfer process is followed by a slow first order chemical reaction or a slow dimerization reaction. We observed the levelling off of i_c/i_a at lower scan rates than $0·05 \sim 0·1$ V s⁻¹. Although more extensive study is necessary to evaluate the kinetic

parameter of the reaction scheme, the present work supports the scheme proposed by Kanzaki *et al.* [7].

3.2. *Chlorine evolution*

One of the electrode materials available for chlorine evolution is carbon. The chlorine evolution on carbon is reversible in LiCl–KCl eutectic [13]. Electrode materials such as platinum and gold are attacked or passivated during chlorine evolution. In view of the chemical and thermal stabilities of oxides, chlorine evolution on conductive oxides such as SnO_2 is of interest in the development of anode materials usable in molten salt systems.

Fig. 4 shows steady-state current versus potential curves obtained at GC and SnO_2 electrodes, where the potential is the value obtained after correcting for the *iR*-drop, which was estimated from the value of electrode resistance measured with an a.c. bridge. Constant currents were increased step-wise, and the electrode potentials were taken after 3 min. At high current densities, gas evolution was observed on both electrodes.

It is obvious that the chlorine evolution on SnO_2 is less reversible than on GC. The increase of polarization at SnO_2 with increasing the current density is quite noticeable in comparison with GC, indicating a different charge transfer mechanism. The large polarization of SnO_2 at high current densities is not attributed to the participation of the mass transfer process, because the diffusion limit is located at a much higher current density as suggested by the results of GC. According to Shams El Din, the concentration polarization in the evolution of chlorine from LiCl–KCl eutectic can be safely set equal to zero [14].

The SnO_2 electrodes used in this work were highly doped specimens whose carrier concentration was $10^{20} \sim 10^{21} \, cm^{-3}$. The flat band potential of the electrode in LiCl–KCl eutectic has been estimated to be -1.29 V versus 1 M Pt(II)/Pt at $450°$ C [1]. Accordingly the band bending is large at the potentials of chlorine evolution, and the space charge barrier is so thin that the electron tunnelling through the barrier must be dominant in the charge transfer process. Judging from the polarization curves in Fig. 4, the exchange current density due to the tunnelling at SnO_2 is lower by one and a half orders than that at GC. It may be possible to apply the theoretical treatment of electron tunnelling proposed by Memming *et al.* [15] for the quantitative interpretation of chlorine and oxygen evolution reactions in SnO_2. Further work is being undertaken.

Acknowledgement

References

[1] I. Uchida, H. Asano and S. Toshima, *J. Electroanalyt. Chem.* **93** (1978) 221.
[2] I. Uchida, K. Niki and H. A. Laitinen, *J. Electrochem. Soc.* **125** (1978) 1759.
[3] I. Uchida, H. Urushibata and S. Toshima, *J. Electroanalyt. Chem.* **96** (1979) 45.
[4] I. Uchida and H. A. Laitinen, *J. Electrochem. Soc.* **123** (1976) 829.
[5] H. A. Laitinen, Y. Yamamura and I. Uchida, *ibid* **125** (1978) 1450.
[6] I. Hodara and H. A. Laitinen, personal communication.
[7] Y. Kanzaki and M. Takahasi, *J. Electroanalyt. Chem.* **58** (1975) 339.
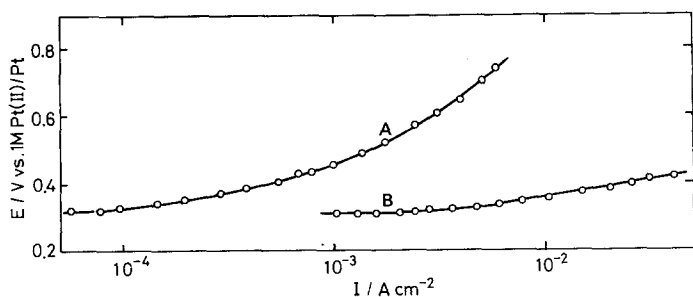[8] R. S. Nicholson and I. Shain, *Analyt. Chem.* **36** (1964) 706.

Fig. 4. Steady-state polarization curves for chlorine evolution in LiCl–KCl eutectic at $450°$ C. (A) SnO_2 electrode, (B) glassy carbon electrode.

[9] C. A. Melendres, J. P. Ackerman and R. K. Steunenberg, *Proceedings of the International Symposium on Molten Salts*, The Electrochemical Society (1976) p. 575.

[10] J. A. Plambeck in A. J. Bard (Ed.), Encyclopedia of Electrochemistry of the Elements. Vol. X, Fused Salts Systems, Marcel Dekker, New York (1976) p. 14.

[11] N. S. Wrench and D. Inman, *J. Electroanalyt. Chem.*, 17 (1968) 319.

[12] Y. Kanzaki, K. Kogawa, S. Yano, O. Matsumoto and M. Takahashi, *Denki Kagaku* 43 (1975) 278.

[13] H. A. Laitinen and J. W. Pankey, *J. Amer. Chem. Soc.* 81 (1959) 1053.

[14] A. M. Shams El Din, *Electrochimica Acta* 4 (1961) 242.

[15] R. Memming and F. Möllers, *Ber. Bunsenges. Phys. Chem.* 76 (1972) 469, 475.